INCT--1/B/00 ISSN 1425-7351

RAPORTY IChTJ. SERIA B nr 1/2000

MULTIVARIATE SIGNAL PROCESSING IN MEASUREMENTS OF RADON AND RADON DAUGHTERS IN AIR

Piotr Urbański, Bronisław Machaj

® INSTYTUT CHEMII I TECHNIKI JĄDROWEJ
INSTITUTE OF NUCLEAR CHEMISTRY AND TECHNOLOGY

WARSZAWA

PLEASE BE AWARE THAT
ALL OF THE MISSING PAGES IN THIS DOCUMENT
WERE ORIGINALLY BLANK

RAPORTY IChTJ. SERIA B nr 1/2000

MULTIVARIATE SIGNAL PROCESSING IN MEASUREMENTS OF RADON AND RADON DAUGHTERS IN AIR

Piotr Urbański, Bronisław Machaj

Warszawa 2000

ADDRESS OF THE EDITORIAL OFFICE

Institute of Nuclear Chemistry and Technology
Dorodna 16, 03-195 Warszawa, POLAND
phone: (+4822) 811 06 56; tlx: 813027 ichtj pl; fax: (+4822) 811 15 32;
e-mail: sekdyrn@orange.ichtj.waw.pl

Papers are published in the form as received from the Authors

UKD: 721.3
INIS: D22
KEY WORDS: MULTIVARIATE PROCESSING, RADON, RADON DAUGHTERS MEASUREMENTS

Wielowymiarowa obróbka sygnału w pomiarach radonu i produktów rozpadu radonu w powietrzu

W komorze radonowej przeprowadzone zostały szerokie pomiary miernika stężenia radonu i miernika produktów rozpadu radonu. Mierzono i rejestrowano "widma" szybkości liczenia impulsów na wyjściu detektora promieniowania. Widma te z kolei poddano wielowymiarowej obróbce z wykorzystaniem techniki regresji głównych składowych oraz badano średni błąd kwadratowy szybkości liczenia impulsów. Stwierdzono, że obróbka regresji głównych składowych usuwa znaczną część fluktuacji szybkości liczenia impulsów będących wynikiem statystyki promieniowania. W wyniku tego maleje błąd przypadkowy szybkości liczenia impulsów. Średni błąd kwadratowy szybkości liczenia impulsów miernika produktów rozpadu radonu jest ok. 3 razy mniejszy, co jest ekwiwalentne z błędami miernika o 9 razy większym przepływie powietrza, jeśli nie jest stosowana obróbka regresji głównych składowych. W przypadku miernika stężenia radonu wzrost czułości jest jeszcze wyższy i wynosi 5 razy.

Multivariate signal processing in measurements of radon and radon daughters in air

Extensive measurements of radon and radon daughters concentration gauge in a radon chamber were carried out. Count rate "spectra" against time at the output of radiation detectors were measured and registered. The count rate spectra were then processed employing Principal Component Regression (PCR). A root mean square error of the count rate was estimated. It was found that PCR processing removes a great part of count rate random fluctuations originating from the radiation statistics that results in a decrease of count rate random error. The root mean square error of count rate in a radon daughter monitor is about 3 times lower, which is equivalent to the error of the gauge with a 9 times higher air flow rate if no PCR processing is used. In case of the radon concentration gauge the increase of sensitivity is even higher and amounts to 5 times.

CONTENTS

1. INTRODUCTION

An important parameter of any gauge for the measurement of concentration of radon or radon decay products in air is the sensitivity of the gauge. The limitation of the sensitivity is imposed by random fluctuations of the measured signal (count numbers) by the measuring head of the gauge. Principal Component Analysis (PCA) applied to the measured signals from a measuring head is able to remove a great part of fluctuations of the signal. It can thus be expected that the application of PCA (multivariate processing) to the signal from the measuring head of radon or radon daughters gauge should also decrease statistic fluctuations of the signal, which will result in an increase of the sensitivity of the gauge. This idea encouraged the present authors to verify the concept of multivariate processing and to assess the eventual increase of sensitivity of such gauges.

2. MULTIVARIATE SIGNAL PROCESSING

Multilinear regression generally can be presented in the form [1-3]:

$$Y = XB + E \tag{1}$$

where: Y is the matrix with n rows and p columns representing p dependent variables, X is the matrix of independent variables with n rows and m columns representing n measured signals (spectra) in m "channels" in case of spectrometric measurements or at m time intervals in case of count rates measured at successive time intervals, E is the matrix with n rows and p columns representing the residual error.

Principal Component Analysis is a method representing the matrix X of independent variables in the form:

$$X = t_1 p_1' + t_2 p_2' + \ldots\ldots + t_a p_a' = TP' \tag{2}$$

where: t are the vectors (scores) with n rows (and 1 column) whose elements are the coordinates of the respective points on the principal component line, p' are the transposed vectors (loadings) with m columns (and 1 row), a is the number of factors (number of principal components) used. The X matrix is replaced by the sum of limited number of $t_i p_i'$ products (usually a few) containing useful information about dependent variables with rejected $t_i p_i'$ with higher indices containing mainly random noise. It can be written from Eq. (2):

$$T = XP \tag{3}$$

where: T is the score matrix with n rows (number of measurements) and a columns (number of principal components employed), X is the matrix of independent variables (measured signals) in Eq. (1) and (2), P is the loading matrix with m rows (number of channels) and a columns (number of principal components).

In the Principal Component Regression (PCR) method, the data matrix X in Eq. (1) is replaced by its score matrix T and the equation relating the dependent variables with independent ones takes the form:

$$Y = TB + E \tag{4}$$

3. SIGNAL PROCESSING OF RADON DAUGHTERS GAUGE

3.1. Measurements with RGR radon daughters monitor

A model of the gauge employing the principle of alpha activity registration at three time intervals was investigated in a radon chamber presented in Fig. 1. A higher or lower concentration of radon in the 0.8 m^3 radon chamber, was realized by circulating the air from the radon chamber through a radon source chamber and through an air filter, in a closed loop. The radon source, a 5 l chamber with an open ^{226}Ra source inside is ensuring a radon concentration of about 9 Bq/cm^3. The Lucas cell was employed to control radon concentration in the radon chamber. Concentration of aerosols in the radon chamber was varied by introducing a cigarette smoke into the radon chamber. A window at the wall of the radon chamber and rubber sleeves (not shown in Fig. 1) allowed to manipulate the investigated model gauge [4], (Fig. 2). The alpha activity of radon decay products deposited within 5 min on the air filter was detected by a semiconductor alpha detector. The pulses after amplification and discrimination were fed to a computer based programmable pulse counter located outside of the radon chamber. The number of counts was measured every minute within 30 min. The counting started parallel with the start of air pumping through the air filter. The count rate "spectra" against time received in such a manner, were used to compute the radon decay products concentration from the following equations [5]:

$$A = \frac{1}{v\varepsilon_1}(2{,}032\ n_1 - 1{,}555\ n_2 + 1{,}179\ n_3) \quad [Bq/m^3] \tag{5}$$

$$B = \frac{1}{v\varepsilon_2}(0{,}4595\ n_1 - 1{,}143\ n_2 + 1{,}807\ n_3) \quad [Bq/m^3]$$

$$C = \frac{1}{v\varepsilon_3}(-0{,}6100\ n_1 + 1{,}143\ n_2 - 0{,}9450\ n_3) \quad [Bq/m^3]$$

$$E = (5.900\,A + 28.56\,B + 21.20\,C)\ 10^{-4} \quad [\mu J/m^3]$$

where: A, B, C, E are the ^{218}Po, ^{214}Pb, ^{214}Bi and alpha potential energy concentrations; v is the air flow rate through an air filter = 2 l/min; ε_1=0.24, ε_2=0.30, ε_3=0.27 are the deposition and detection efficiencies of radon decay products; n_1, n_2, n_3 are the count numbers at time interval t_1=1-7 min, t_2=8-20 min, t_3=21-30 min, respectively. The same spectra are used for multivariate processing. Measurements of 49 spectra were carried out at different radon daughters concentrations in the radon chamber (different radon concentration and smoke aerosols concentration) - the matrix X in Eq. (1)-(3). The measured spectra (the X matrix raw data) are shown in Figs. 3 and 4.

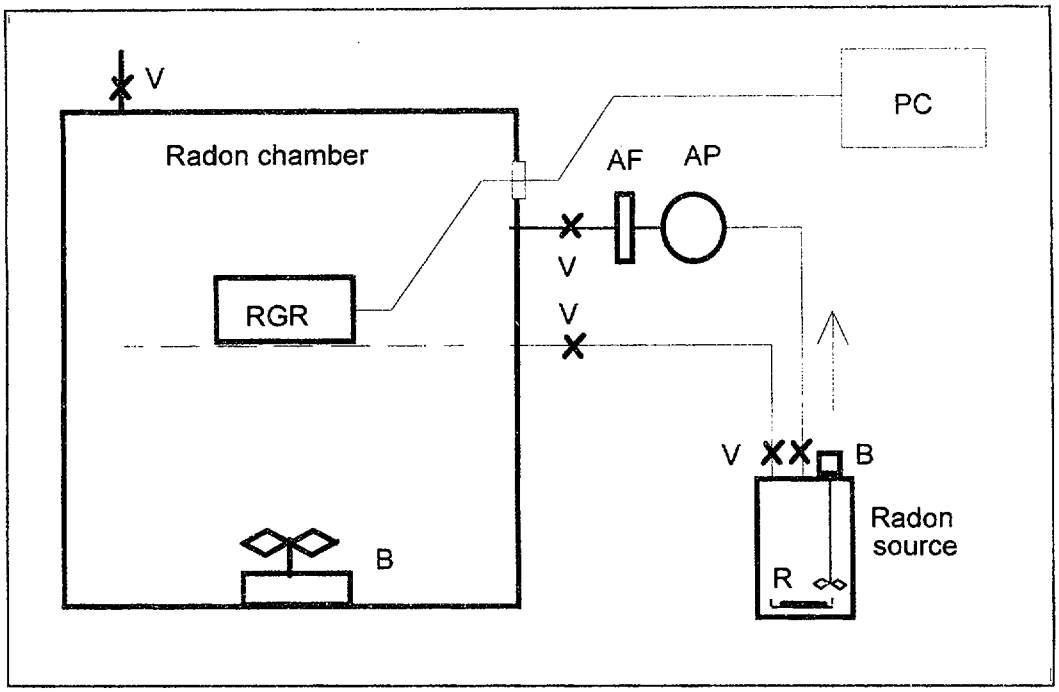

Fig. 1. Block diagram of the radon chamber measuring set: RGR - model gauge under investigation, B - air blower, V - stop valves, AF - air filter, AP - air pump, R - open ^{222}Ra source, PC - programmable counter.

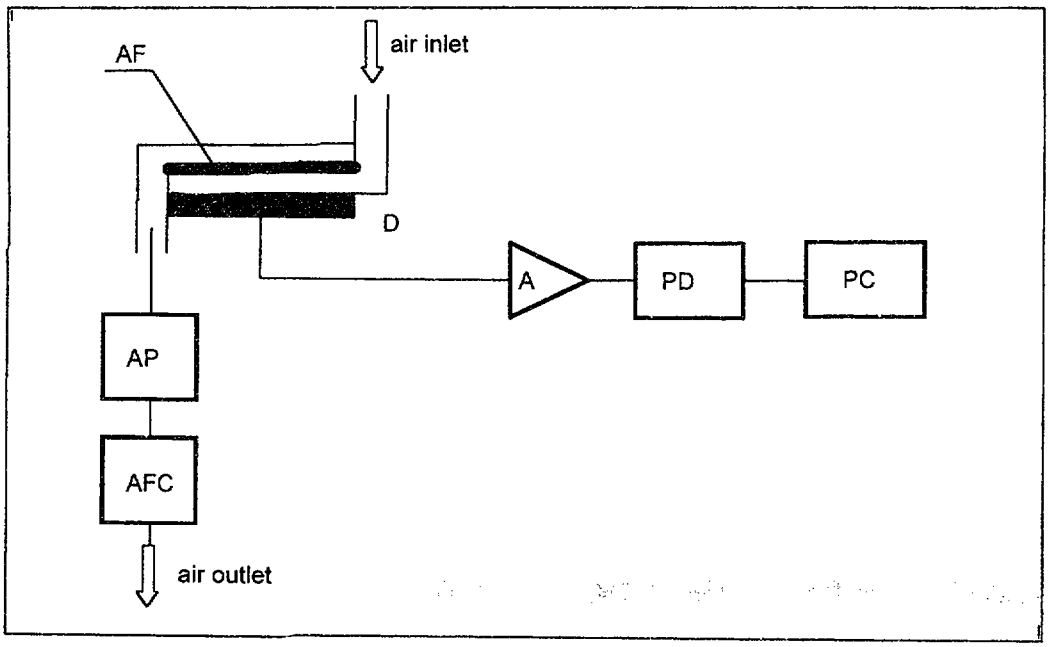

Fig. 2. Block diagram of the model gauge: AF - air filter, D - alpha detector, AP - air pump, AFC - air flow controller, A - pulse amplifier, PD - pulse discriminator, PC - programmable counter.

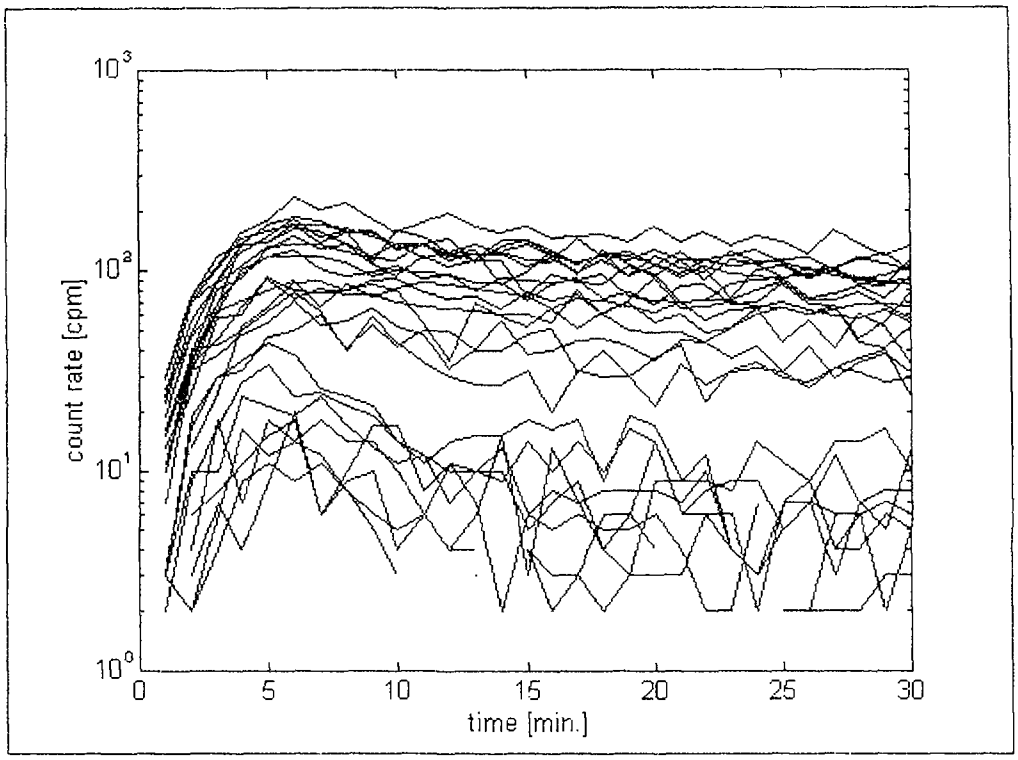

Fig. 3. Measured 25 count rate spectra at low radon daughters concentrations with large relative count rate fluctuations.

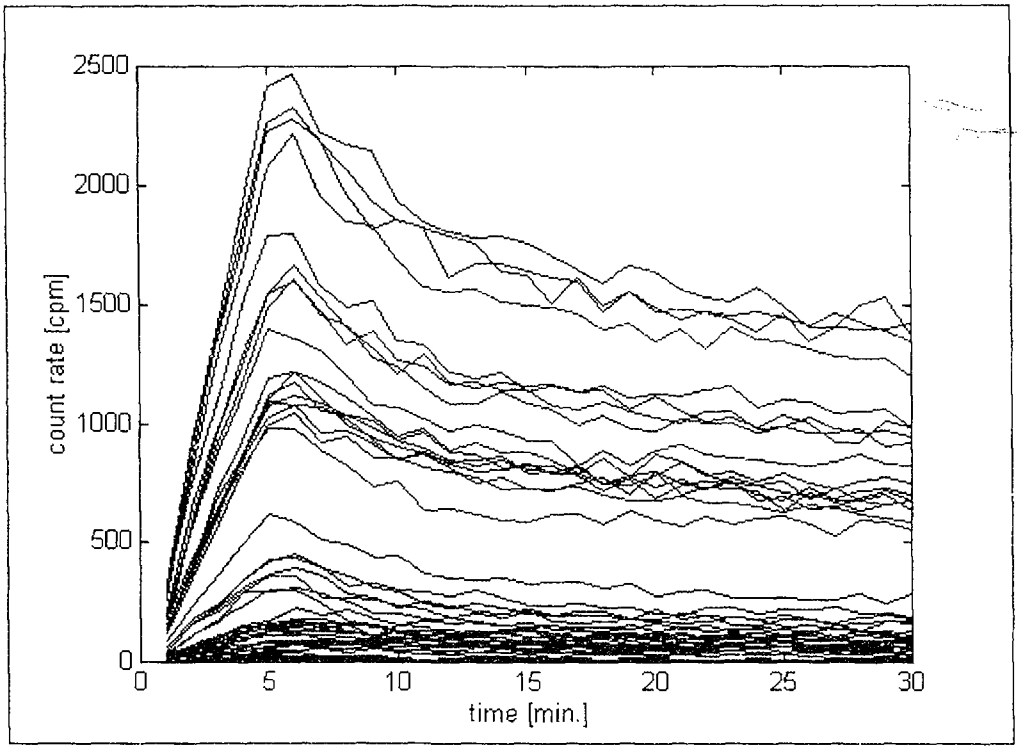

Fig. 4. Measured 49 count rate spectra at low and at high radon daughters concentrations.

3.2. Random errors of raw data

In a decay series of a radionuclide A into its daughters A→B→C→... the number of atoms of the nuclide A, B, C is given by the relations [6]:

$$A = A_o e^{-\lambda_A t} \tag{6}$$

$$B = B_o e^{-\lambda_B t} + A_o \frac{\lambda_A}{\lambda_B - \lambda_A}(e^{-\lambda_A t} - e^{-\lambda_B t})$$

$$C = C_o e^{-\lambda_C t} + B_o \frac{\lambda_B}{\lambda_C - \lambda_B}(e^{-\lambda_B t} - e^{-\lambda_C t}) + A_o(h_A e^{-\lambda_A t} + h_B e^{-\lambda_B t} + h_C e^{-\lambda_C t})$$

where:

$$h_A = \frac{\lambda_A}{\lambda_C - \lambda_A}\frac{\lambda_B}{\lambda_B - \lambda_A}; \quad h_B = \frac{\lambda_A}{\lambda_A - \lambda_B}\frac{\lambda_B}{\lambda_C - \lambda_B}; \quad h_C = \frac{\lambda_A}{\lambda_A - \lambda_C}\frac{\lambda_B}{\lambda_B - \lambda_C};$$

A_O, B_O, C_O is the number of atoms of nuclide A=^{218}Po, B=^{214}Pb, C=^{214}B (^{214}Po) at time t=0; $\lambda=0.693/T_{1/2}$ is the decay constant of a nuclide; $T_{1/2}$ is the half period of a nuclide. The activity of the nuclides A, B, C is:

$$A_a = \lambda_A A \tag{7}$$
$$B_a = \lambda_B B$$
$$C_a = \lambda_C C$$

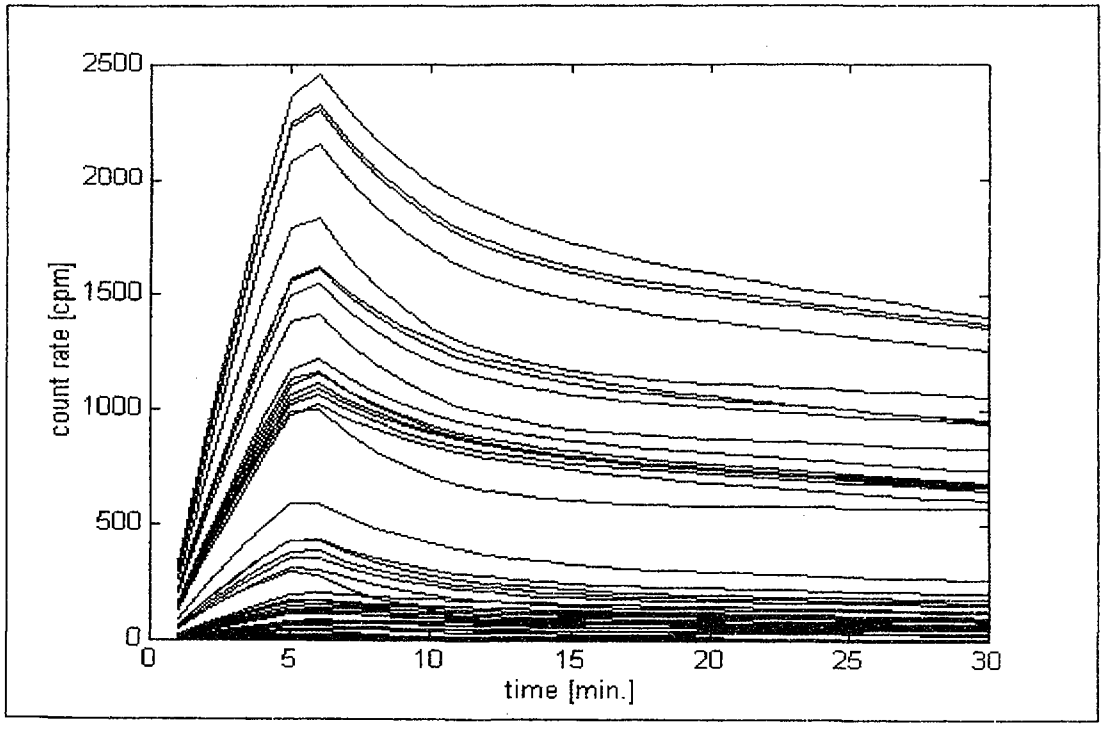

Fig. 5. Simulated count rate from RGR radon daughter monitor at low and high radon daughters concentrations.

To simulate the continuous process of deposition of the radon daughters on an air filter, the activity of A, B, C nuclides deposited on the air filter within 1/10 min was computed against time at 1/10 min intervals and then such spectra were summed with a 1/10 min delay. Introducing into Eq. (6) the number of atoms of A, B, C nuclides resulting from the measured concentration of A, B, C according to Eq. (5), simulated spectra were computed and are presented in Figs. 5 and 6.

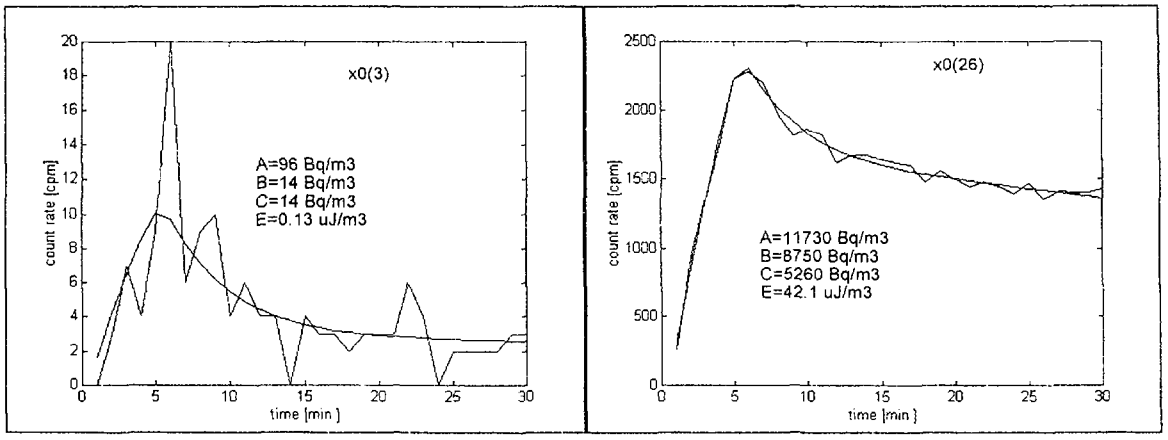

Fig. 6. Measured (broken line) and simulated (continuous line) count rates at low (left) and high (right) concentrations of radon daughters (at high smoke aerosols concentration). Employing Eq. (6) and (7) concentrations A, B, C and E shown in the diagrams were computed.

Root mean square error (RMSE) of the measured (raw) count rate x_0 due to the statistics of radioactive disintegration at three time intervals t_1=1-7 min, t_2=8-20 min, t_3=21-30 min was computed with respect to the simulated count rate from the relation:

$$\mathrm{RMSE} = \sqrt{\frac{\sum_i (x_i - \bar{x}_i)^2}{n}} \qquad (8)$$

where: $\bar{x}$ is the simulated count rate, x is the measured count rate, n is the number of readings at time intervals (n=7, 13 and 10 at t_1, t_2, t_3 intervals, respectively). RMSE of 49 measured count rate spectra are given in Table 1.
The mean count rate and RMSE in Table 1 were computed employing a MATLAB program given in Appendix 1.

3.3. Random errors of PCR processed data

Employing Multivariate Analysis [7] the 49 measured raw spectra, x_0, of count rates of the RGR radon daughters monitor were processed employing the MATLAB Principal Component Regression program based on PCA. It was found that the shape of the measured (raw) count rate spectra is sufficiently well represented by two principal components and the fluctuations of the count rate spectra are greatly reduced. The PCR processed spectra with two principal components were received from MATLAB:

Table 1. Mean count rate and RMSE of count rate of raw data.

Measurement number	n_1 cpm	n_2 cpm	n_3 cpm	RMSE(n_1) cpm	RMSE(n_2) cpm	RMSE(n_3) cpm
1	7	3.38	1.9	1.86	2.56	2.32
2	8.86	6	3.2	2.68	2.22	2.34
3	7	4.23	2.7	4.41	1.69	1.46
4	50	32.85	31.6	7.32	6.6	4.74
5	95.29	114.23	92.9	6.65	13.35	5.2
6	80	86.38	70.5	5.52	7.38	11.04
7	58.14	75.62	62.4	10.23	5.01	4.46
8	27.71	11.23	6	3.05	3.1	1.84
9	139	165.15	137.3	13.82	14.46	11.48
10	114.43	127.31	104.7	15.07	8.69	11.22
11	119.57	126.92	106.8	6.4	11.1	7.48
12	104.29	115.23	96.2	12.19	8.06	11.64
13	121	125.69	105.1	8.73	13.07	9.78
14	107.86	126.77	103.1	11.57	18.63	12.74
15	90.43	101.77	80.5	7.86	11.43	10.6
16	80.57	90.38	72.2	5.71	6.69	7.24
17	47.86	76.62	65.8	9.04	9.19	4.07
18	44.14	46.15	37.4	5.45	6.7	4.7
19	34.57	42.69	31	4.55	6.23	4.99
20	19.86	15.85	11.4	3.5	3.87	2.99
21	15.86	12.31	8.1	3.35	3.31	2.77
22	9.14	9.23	6.3	3.24	3.27	2.56
23	11.29	8.92	6.1	4.4	3.5	1.81
24	58.29	63.08	55.2	6.99	11.05	7.97
25	57.43	64.08	49.8	6.24	6.76	8.8
26	1263.86	1244.54	1086.5	41.77	34.01	37.11
27	1467.43	1556.92	1321.2	37.85	31.23	32.89
28	1571.71	1677.92	1422.5	49.36	53.19	38.43
29	1583.57	1704.54	1442.7	24.92	43.14	22.89
30	1668	1807.85	1493.2	34.92	42.54	53.07
31	204	89.46	52.8	18.17	8.31	7.42
32	693.57	648.77	580.3	14.24	27.15	24.09
33	976.71	971.85	851.5	25.31	33.32	21.13
34	1061.14	1120.08	972.7	32.59	36.72	18.24
35	1106	1196.69	998.9	33.35	45.93	35.44
36	1102.86	1170.69	998.2	26.11	30.65	24.84
37	415.86	362.69	277.4	14.86	16.98	14.61
38	301.29	269.69	214.8	13.01	16.34	13.02
39	267.57	222.92	174.2	11.8	12.04	15.05
40	300.57	243	187.5	15.42	16.14	10.12
41	246.86	205.62	162.6	17.37	11.3	16.49
42	217	169.23	130	21.08	10.03	11.66
43	829.14	907.38	773.3	28.55	33.99	23.41
44	764	862.69	730.5	31.35	44.7	40.91
45	755.14	830.38	699.1	20.9	28.37	31.49
46	795.43	838.31	704.1	33.74	27.7	24.86
47	724.43	801.85	685.5	17.23	35.03	25.52
48	783	857.92	722.9	23.73	20.43	20.55
49	689.43	771.54	642.4	21.51	16.24	12.99

[t,p,b,ssq,eigs]=pcr(x_0,y_0,2,0); (9)
tp2=t*p'

where: tp2 is the the matrix of PCR processed x_0 raw data covering 100% variance in block y_0 (dependent variables) and 99.13% of variance in block x_0. The PCR processed spectra are shown in Figs. 7-9. Comparing Figs. 7 and 8 with Figs. 3 and 4 it can be easily noticed that the fluctuations of the count rates are considerably decreased. RMSE of PCR processed spectra were also computed according to Eq. (8) with respect to simulated count rate spectra. The computations were carried out, employing the MATLAB program given in Appendix 2, and are presented in Table 2.

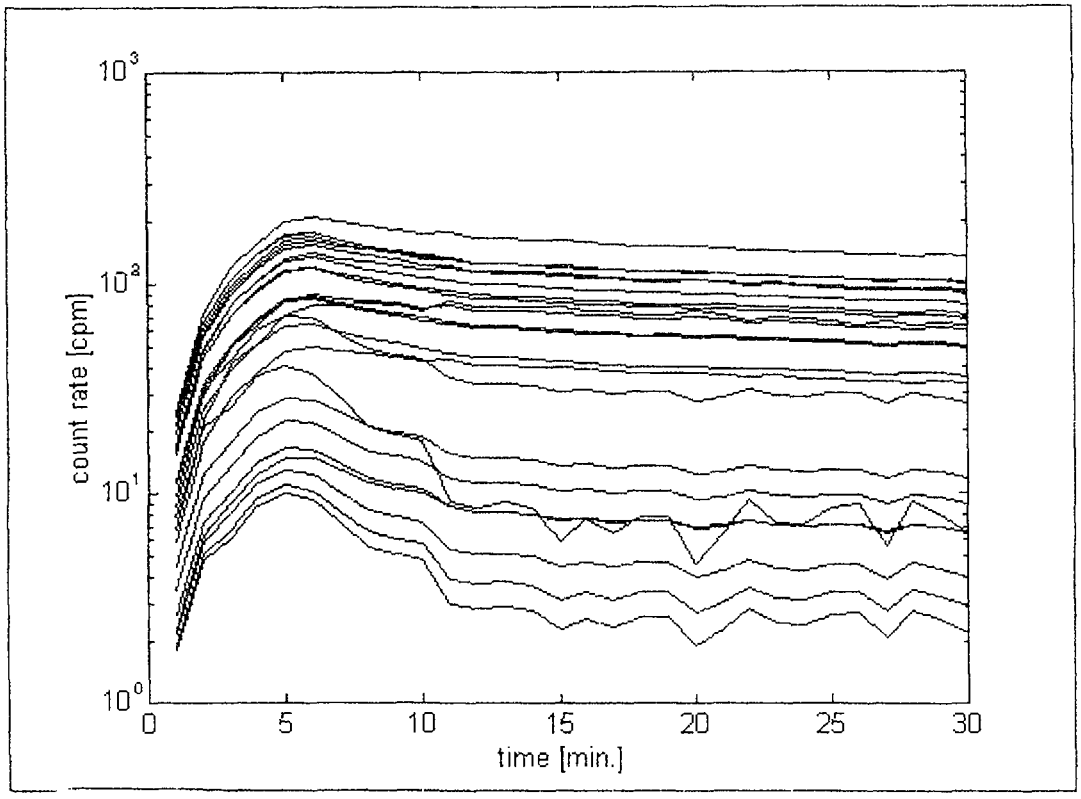

Fig. 7. PCR processed 25 count rate spectra at lower radon daughters concentration.

Average count rates and the average RMSE of raw and PCR processed spectra are given in Table 3. The data are divided into two groups. One group contains the measurements (1-25) at a low radon daughters concentration, the other group contains all the measurements (1-49) at low and high radon daughters concentrations. The group at the low radon daughters concentration is of special interest as the decrease of about 3 times of RMSE error of PCR processed raw data is equivalent to a 3 times higher sensitivity of the gauge. Such an increase of sensitivity without PCR processing would require a $3^2=9$ increase of the air flow rate through the filter.

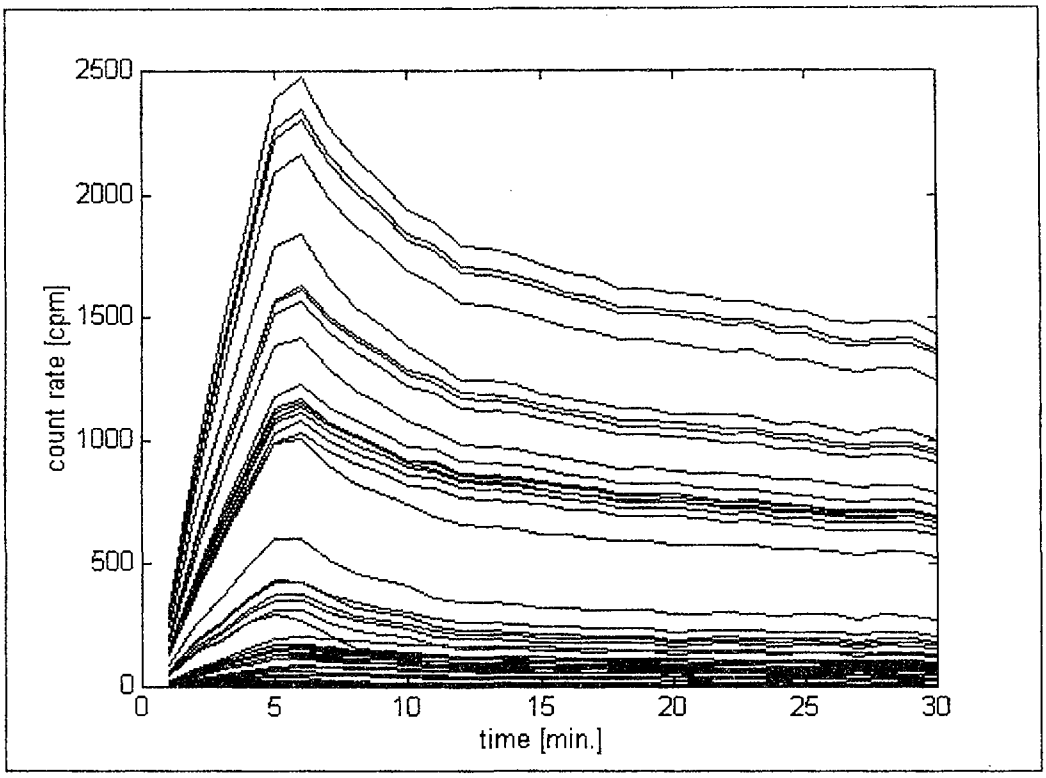

Fig. 8. PCR processed 49 count rate spectra at low and at high radon daughters concentrations.

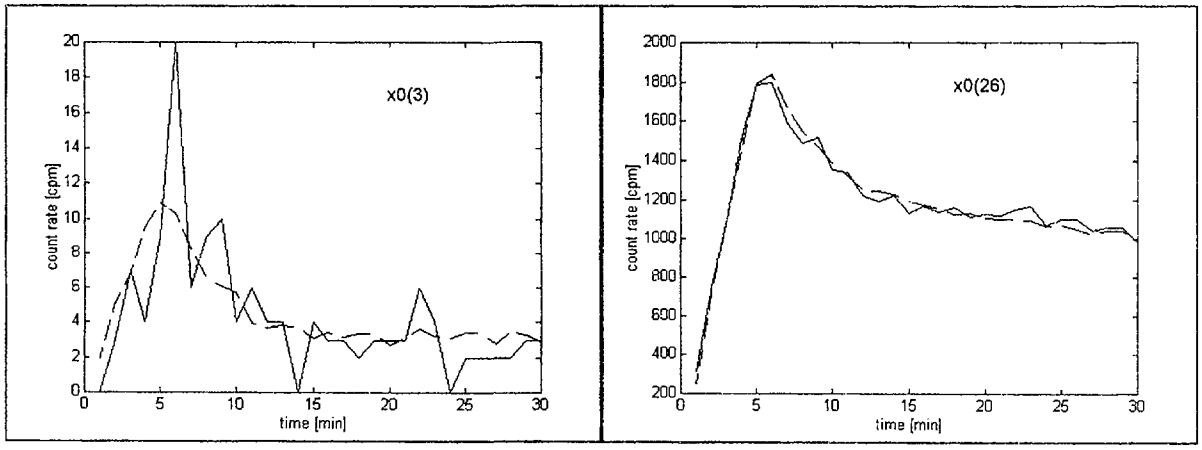

Fig. 9. Measured (raw) - broken line, and PCR processed data - dotted line count rate spectra at low radon daughters concentration - the left diagram, and at high radon daughters concentration - the right diagram.

Table 2. Mean count rate and RMSE of PCR processed data.

Measurement number	n_1 cpm	n_2 cpm	n_3 cpm	RMSE(n_1) cpm	RMSE(n_2) cpm	RMSE(n_3) cpm
1	6.84	3.18	2.49	0.62	0.78	0.54
2	8.95	5.47	4.43	0.59	1.06	1.21
3	7.55	4.05	3.24	0.67	0.42	0.59
4	49.35	35.02	28.79	1.35	2.81	3.62
5	92.98	112.19	95.71	3.57	3.68	3.13
6	80.83	85.29	72.22	1.42	2.82	1.57
7	58.83	74.11	63.36	1.49	2.15	1.59
8	28.32	10.23	7.67	1.68	2.17	2.1
9	138.55	164.19	139.94	2.31	2.55	3.16
10	113.1	125.09	106.21	2.06	2.71	2.01
11	119.91	126.14	106.78	1.25	1.18	1.02
12	103.85	115.06	97.7	1.35	1.25	1.71
13	120.35	125.94	106.58	1.21	1.22	1.82
14	108.12	125.14	106.52	9.89	12.26	4.19
15	90.71	99.74	84.66	1.62	2.77	4.5
16	81.93	88.57	75.11	1.98	2.34	3.1
17	50.18	76.65	66.1	3.27	2.37	1.93
18	44.64	45.09	38.08	0.85	1.19	0.87
19	33.84	40.9	34.89	1.85	2.66	4.12
20	19.99	15.19	12.56	0.63	1.02	1.24
21	15.33	11.58	9.57	0.85	1.15	1.52
22	10.37	8.4	6.99	1.4	0.91	0.78
23	11.49	8.46	6.98	0.47	0.68	0.93
24	59.89	63.3	53.61	1.83	0.9	1.79
25	58.19	61.93	52.46	1.46	2.62	2.86
26	1258.17	1256.44	1060.28	11.9	17.73	32.17
27	1467.67	1557.65	1319.38	14	12.09	12.8
28	1560.58	1680.05	1424.26	18.89	14.09	13.43
29	1588.96	1704.16	1444.37	17.32	13.61	13.43
30	1676.16	1789.1	1515.94	21.52	26.11	27.93
31	206.45	84.82	65.08	10.5	14.29	14.5
32	692.73	662.26	557.28	7.74	17.23	27.36
33	970.78	985.18	832.21	10.95	16.63	24.23
34	1065.1	1130.51	957.58	12.51	14.99	18.99
35	1103	1192.91	1011.56	12.01	11.88	16.05
36	1098.56	1171.85	992.89	11.31	9.25	11.1
37	419.76	351.31	292.83	10.48	16.25	17
38	299.92	266.02	222.69	4.77	7.47	8.91
39	265.52	219.84	183.09	6.18	8.34	9.81
40	303.21	237.53	196.95	7.43	10.4	11.08
41	248.08	201.65	167.7	5.02	7.51	6.46
42	220.25	165.55	136.79	6.35	7.7	8.24
43	830.52	910.58	772.76	9.64	8.51	7.17
44	765.83	862.22	732.82	32.98	31.1	23.55
45	754.41	829.03	703.65	8.53	7.62	7.99
46	794.28	838.26	709.79	7.46	7.05	8.74
47	727.16	802.51	681.31	9.21	7.37	7.55
48	783.17	854.97	725.38	8.64	8.1	7.12
49	697.83	764.93	649.15	12.44	10.06	9.61

Table 3. Average count rate and average RMSE of raw and PCR processed spectra.

Measurement number	n_1 cpm	n_2 cpm	n_3 cpm	RMSE(n_1) cpm	RMSE(n_2) cpm	RNSE(n_3) cpm
1-25 raw	60.38	66.08	53.93	6.79	7.52	6.25
1-25 PCR	60.57	65.24	55.31	1.83	2.23	2.08
1-49 raw	434.66	452.75	381.08	15.90	17.62	14.95
1-49 PCR	434.94	452.05	382.42	6.60	7.37	8.50

1-25 measurement number: A=0-873 Bq/m^3, B=0-797 Bq/m^3, C=0-1046 Bq/m^3, E=0.11-3.75 uJ/m^3.
1-49 measurement number: A=0-11730 Bq/m^3, B=0-9180 Bq/m^3, C=0-10460 Bq/m^3, E=0.11-53.7 μJ/m^3.

3.4. PCR processing of simulated raw data

Employing the matrix of the 49 simulated count rate spectra described in section 3.2, random fluctuations with a normal distribution were added to the simulated data with the count rate amplitude $\pm n^{0.5}$, see MATLAB program in Appendix 3. Fig. 10 illustrates the simulated and measured count rate spectra at low and high radon daughters concentrations. The achieved in such a manner spectra were then PCR processed with 2, 3 and 4 principal components (Appendix 4). It was found that PCR processing with 2 principal components satisfactorily represents the shape of the measured (raw) spectra and covers 100% of y_o variance and 99.15%. RMSE with the two principal component PCR processing are shown in Table 4.

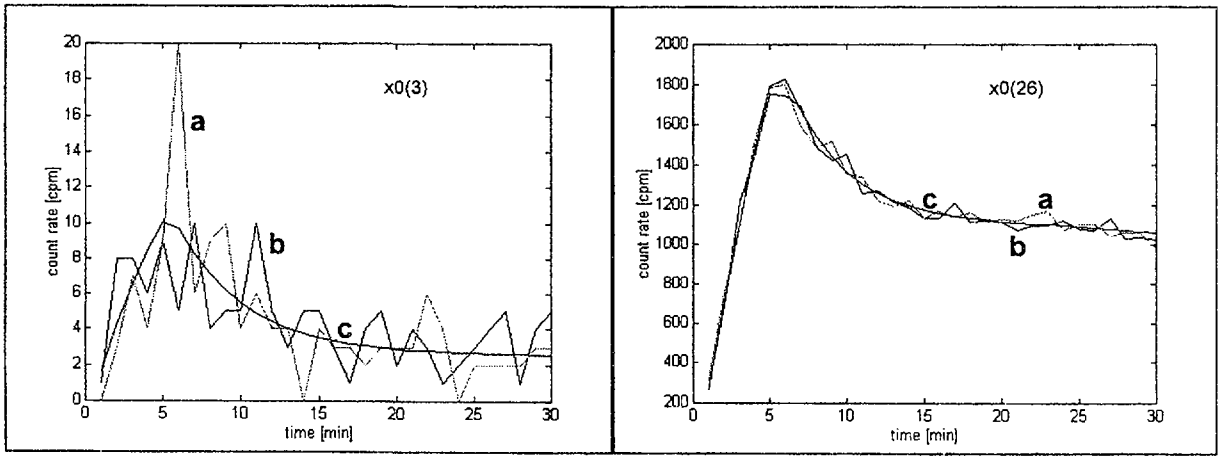

Fig. 10. Simulated and measured count rate spectra at low (left) and high (right) radon daughters concentration: a - measured spectrum, b - simulated spectrum with random error added, c - simulated spectrum.

The last two rows of Table 4 give an average value of count rate and RMSE at low and high radon daughters concentrations. The average RMSE of the spectra with simulated random fluctuations are comparable with the average RMSE of the measured (raw) and PCR pro-

Table 4. Mean count rates and RMSE of count rate of simulated spectra with simulated fluctuations with respect to simulated spectra.

Measurement number	n_1 cpm	n_2 cpm	n_3 cpm	RMSE(n_1) cpm	RMSE(n_2) cpm	RMSE(n_3) cpm
1	6.6	3.49	2.88	0.76	0.55	0.93
2	8.01	6.1	5.13	1.16	0.79	1.89
3	7.13	4.07	3.38	0.29	0.38	0.76
4	49.85	34.31	28.69	1	2.77	3.55
5	101.23	112.76	95.81	5.8	2.87	3.23
6	81.45	86.86	73.72	1.09	1.66	2.97
7	53.47	73.61	62.84	5.33	3.31	1.37
8	26.77	10.36	8.38	1.64	1.96	2.9
9	147.53	167.94	142.77	9.04	3.44	5.6
10	116.42	127.57	108.35	2.32	1.58	3.94
11	124.76	125.82	106.62	5.53	1.87	1.58
12	102.44	112.05	95.16	2.6	3.59	1.57
13	125.58	126.07	106.82	4.89	1.47	2.36
14	119.49	133.31	113.27	3.35	4.36	4.02
15	94.26	98.74	83.76	4.22	3.41	3.88
16	82.51	89.27	75.79	2.2	1.86	3.79
17	45.47	75.1	64.34	3.11	3.03	2.25
18	41.54	45.62	38.75	2.85	1.24	1.45
19	35.36	41	34.87	1.13	2.52	4.1
20	18.33	15.54	13.1	1.72	0.91	1.78
21	14.68	10.92	9.16	1.49	1.61	1.24
22	9.21	8.27	6.99	0.44	1.02	0.82
23	11.02	8.39	7.05	0.47	0.7	1.05
24	57.6	63.87	54.26	1.14	1	1.18
25	55.14	60.9	51.74	2.97	3.73	2.26
26	1257.71	1256.01	1064.02	13.47	19.5	28.22
27	1476.96	1556.4	1320.46	15.05	13.53	14.05
28	1576.63	1667.42	1414.79	13.85	17.86	16.76
29	1579.71	1704.09	1446.66	15.89	15.74	14.42
30	1659.04	1787.02	1517.01	20.69	29.98	30.39
31	205.43	85.05	69.15	8.77	13.3	19.82
32	682.38	655.46	554.64	14.13	13.94	28.68
33	988.38	985.47	834.8	14.92	19.63	21.56
34	1064.23	1118.26	948.67	9.78	12.11	26.15
35	1099.19	1189.65	1010.03	13.41	14.57	15.64
36	1099.22	1163.72	987.44	10.68	12.3	14.76
37	415.82	348.81	293.89	9.05	17.27	20.19
38	299.3	265.48	224.09	4.73	7.14	11.31
39	271.95	219.12	184.36	5.58	7.88	12.53
40	291.39	231.56	194.73	12.22	14.12	11.08
41	250.52	199.49	167.78	5.88	8.82	8.49
42	215.96	167.46	140.7	4.14	6.36	12.5
43	806.12	901.24	765.81	26.76	12.12	10
44	745.9	839.92	713.83	11.98	11.65	7.16
45	773.27	814.75	691.24	19.77	17.75	11.56
46	797.23	837.32	710.32	6.66	7.56	10.09
47	718.32	804.35	683.5	11	8.91	6.25
48	786.22	857.86	728.49	8	8.36	8.96
49	710.61	767.69	651.75	22.48	8.96	12.29
1-25	61.43	65.68	55.74	2.66	2.07	2.42
1-49	434.84	450.32	381.87	7.46	7.57	8.84

cessed spectra (Table 3). This means that the raw spectra can be replaced by the simulated ones with satisfactory accuracy.

4. SIGNAL PROCESSING OF RADON IN AIR GAUGE

4.1. PCR processed Lucas chamber count rate spectra

A gauge for the measurement of radon concentration in air, employing a Lucas cell as detector of alpha radiation originating from radon and radon decay products, was investigated. A series of count rate spectra against time from the Lucas cell were measured in a measuring arrangement (Fig. 1) by means of an electronic measuring circuit described in [8,9]. The Lucas cell ϕ54x74 mm was used in these investigations. The radon concentration y in radon chamber was computed from the relation:

$$y = \frac{n}{60}\frac{1000}{v}\frac{1}{3\varepsilon k} \quad [Bq/m^3] \tag{10}$$

where: n is the count rate measured in the period 161-180 min after the radon had been introduced into the Lucas cell, cpm, v=0.17 l, the Lucas cell volume, ε=0.78, the alpha detection efficiency of the Lucas cell, k=0.9967, the coefficient taking into consideration decrease of radon activity at the time of measurement and incomplete radiation equilibrium in the radon cell. The measured (raw) spectra count rate are shown in Fig. 11.

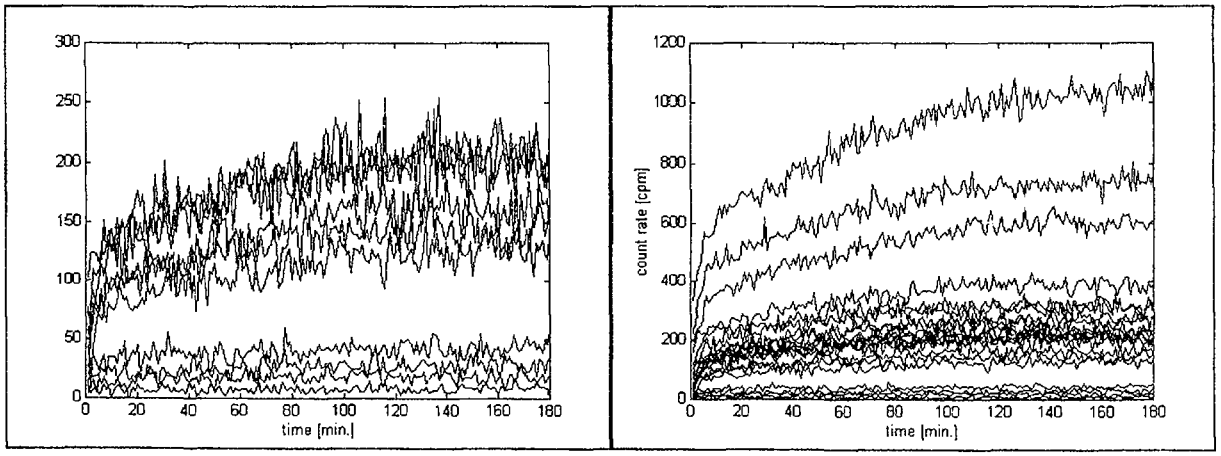

Fig. 11. Count rate spectra of Lucas cell at low (left) and low together with high radon concentrations (right).

To assess random root mean square error resulting from the statistical fluctuations of count rate, first the simulated count rate spectra were computed employing relations describing a decay series of radionuclide A→B→C→D ..... [6]. The simulated count rate spectra are shown in Figs. 12 and 13. RMSE of the measured count rate spectra was computed

with respect to the simulated count rate spectra according to Eq. (8), see Appendix 5. The results of computations are given in Table 5.

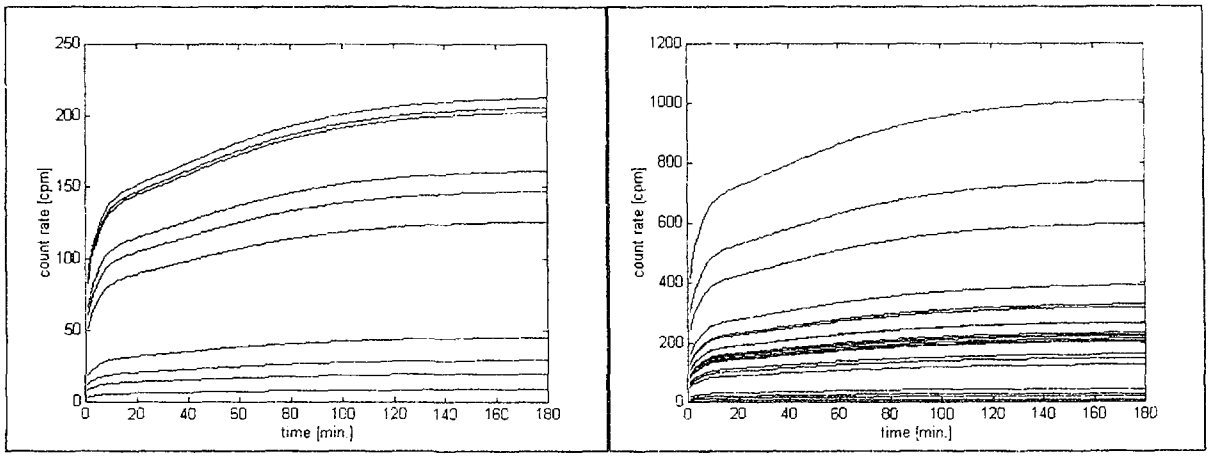

Fig. 12. Simulated spectra of Lucas cell at low (left) and low together with high radon concentrations (right).

It was found that the PCR processed count rate spectra with one principal component fairly well represent the shape of the measured (raw) count rate spectra eliminating a great part of the random fluctuations due to the statistics of radiation. The PCR processed spectra are shown in Fig. 14 and RMSE computed (Appendix 6) are given in Table 6.

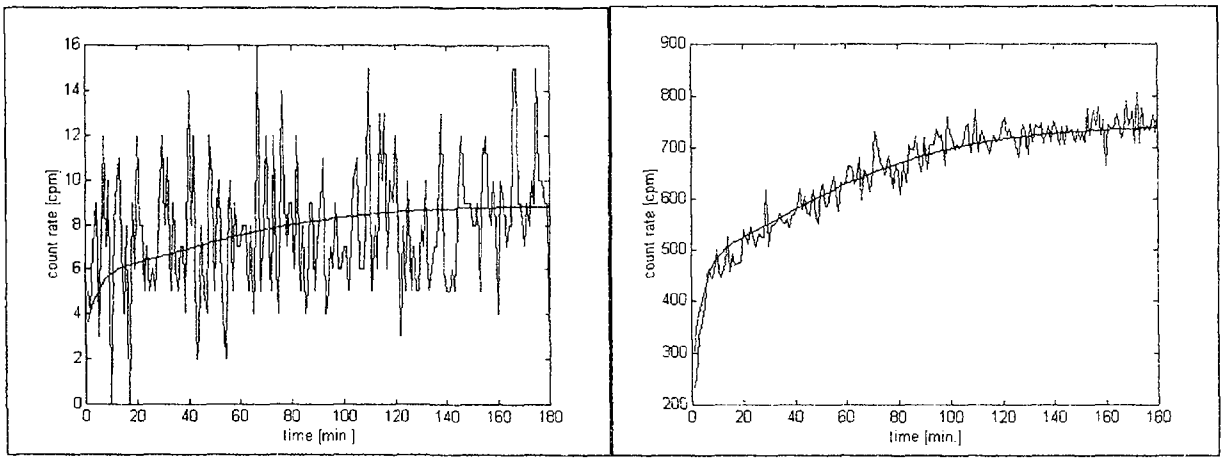

Fig. 13. Measured (broken line) and simulated (continuous line) count rate spectra at low (left) and high (right) radon concentrations.

Comparing the last two rows of Table 5 and Table 6, it can be seen that PCR processing of the Lucas cell raw data decreases nearly 10.34/2.18≅5 times RMSE when the count rate is registered in the period 161-180 min, after the radon has been introduced into the Lucas cell. Fig. 15 shows the estimated radon concentration versus the measured one of PCR processed count rate spectra. RMSE of the estimated concentration with respect to the measured (calibration) one is 2.7% (Appendix 7).

Table 5. Mean count rates and RMSE of count rate of measured (raw) count rate spectra with respect to simulated spectra. Last two rows contain average values.

Measurement number	n(1-10) channel cpm	n(161-180) channel cpm	n(1-180) channel cpm	RMSE (1-10) channel cpm	RMSE (161-80) channel cpm	RMSE (1-180) channel cpm
1	6.4	9.4	7.79	3.6	2.96	2.91
2	11.8	18.15	17.67	4.08	5.35	4.47
3	21.8	28.4	26.04	5.58	5.7	5.29
4	29.7	44.95	39.99	7.31	5.2	6.57
5	73.1	126.55	110.86	11.51	9.63	11.62
6	81.5	141.45	129.72	10.23	14.46	11.23
7	62.4	160.65	141.97	35.33	14.23	15.33
8	103.3	203	178.58	20.04	17.18	15.28
9	126.3	203	181.44	15.18	14.14	14.22
10	94.7	207.05	187.38	35.6	14.53	17.83
11	136.7	221.25	195.92	17.81	14.27	15
12	125.3	230.55	200.18	12.5	15.02	15.51
13	98.1	222.7	205.02	39.75	16.76	18.32
14	121.4	270.8	234.72	41.49	14.16	17.68
15	126.1	263.1	235.67	33.68	16.53	17.77
16	160.1	312.55	280.79	27.87	19.59	18.64
17	222	310.9	288.7	43.74	25.23	22.74
18	191.4	385.85	344.96	47.03	19.43	22.62
19	288	600.75	524.47	53.8	17.45	27.95
20	388.8	747.8	650.67	44.55	27.96	28.8
21	502.9	1046.35	891.74	73.88	51.79	43.73
1-10	61.10	114.26	102.14	14.85	10.34	10.47
11-21	214.62	419.33	368.44	39.65	21.65	22.62

1-10 measurement number: radon concentration = 405-8790 Bq/m^3.
11-21 measurement number: radon concentration = 9590-45350 Bq/m^3.

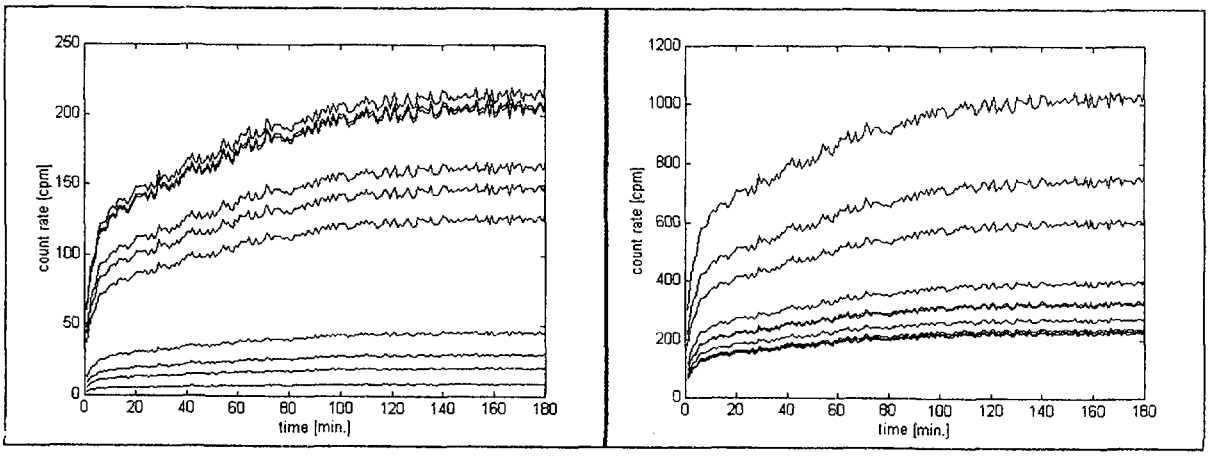

Fig. 14. PCR processed raw count rate spectra at low (left) and high (right) radon concentrations.

Table 6. Mean count rate and RMSE of PCR processed data.

Measurement number	n(1-10) channel cpm	n(161-180) channel cpm	n(1-180) channel cpm	RMSE (1-10) channel cpm	RMSE (161-80) channel cpm	RMSE (1-180) channel cpm
1	4.43	8.81	7.67	0.62	0.13	0.25
2	10.11	20.09	17.5	1.34	0.31	0.53
3	14.9	29.6	25.8	1.98	0.45	0.79
4	22.8	45.31	39.48	3.12	0.66	1.25
5	63.86	126.9	110.58	8.09	2.31	3.32
6	74.6	148.23	129.17	9.57	2.55	3.88
7	82.32	163.59	142.55	9.9	3.72	4.41
8	103.09	204.86	178.52	12.84	4	5.38
9	104.24	207.14	180.51	13.48	3.46	5.43
10	108.17	214.94	187.3	13.49	4.18	5.65
11	112.51	223.58	194.83	14.59	3.69	5.87
12	115.28	229.08	199.63	14.63	4.13	5.99
13	118.61	235.7	205.4	14.53	4.96	6.26
14	135.87	269.98	235.27	16.58	5.76	7.18
15	135.99	270.24	235.49	17	5.19	7.09
16	161.94	321.8	280.43	20.33	6.08	8.43
17	164.93	327.74	285.6	22.27	4.82	8.86
18	199.23	395.89	344.99	24.68	7.92	10.43
19	303.34	602.78	525.28	37.24	12.54	15.97
20	375.4	745.96	650.05	46.99	14.25	19.57
21	515.85	1025.05	893.26	63.27	21.42	27.17
1-10	58.85	116.95	101.91	7.44	2.18	3.09
11-21	212.63	422.53	368.20	26.55	8.25	11.16

1-10 measurement number: radon concentration = 405-8790 Bq/m^3.
11-21 measurement number: radon concentration = 9590-45350 Bq/m^3.

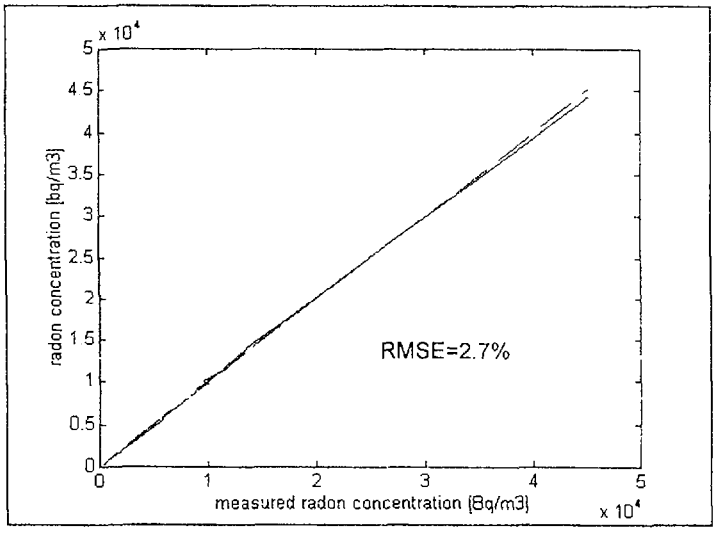

Fig. 15. Estimated radon concentration (continuous line) against measured concentration (dotted line).

4.2. Count rate spectra with high background level

It is known that radon detectors registering the alpha radiation from radon decay products, after a certain time, show an increased background due to the long lived radon decay

Table 7. Measured and estimated radon concentrations from PCR processed raw spectra.

Item	y_o measured Bq/m^3	y_{est} from x_o Bq/m^3	y_{est} from (x_o+bknd) Bq/m^3	$y_{est} \pm std(y_{est})$ from (x_o+bknd) and corrected b_o Bq/m^3
	1	2	3	4
1	405	263	666	251 ± 2.0
2	783	752	1138	739 ± 1.2
3	1224	1165	1536	1152 ± 1.7
4	1937	1846	2193	1833 ± 1.8
5	5757	5384	5610	5371 ± 2.7
6	6134	6309	6502	6297 ± 3.9
7	6962	6975	7141	6964 ± 4.9
8	8798	8764	8870	8755 ± 5.0
9	8792	8863	8968	8855 ± 5.3
10	8979	9201	9292	9195 ± 3.6
11	9589	9576	9657	9574
12	9992	9814	9886	9814
13	9651	10102	10165	10104
14	11741	11588	11598	11591
15	11400	11599	11609	11601
16	13551	13835	13768	13840
17	13500	14092	14019	14099
18	16758	17047	16867	17053
19	26037	26018	25530	26024
20	32410	32227	31526	32237
21	45348	44329	43208	44339
b_o	-	-118.7	-118.7	-858.7

bknd - background spectrum (rk42).
Column 1 - calibration values.
Column 2 - estimated values from pcr(x,y,1) and $y_{est}=b_o+x_o b'$ (Appendix 7), b_o= -118.7.
Column 3 - estimated (computed) values from $y_{est}=b_o+(x_o+bknd)b'$, b_o= -118.7, where x_o is replaced by $z_o=x_o+bknd$ according to Appendix 9, the same b' regression coefficients are used.
Column 4 - estimated values from $y_{est}=b_o+(x_o+bknd)b'$, b_o= -858.7. Processing as for column 3 with corrected value of b_o (Appendix 8).

products ^{210}Pb, ^{210}Bi, ^{210}Po. To verify the behavior of Lucas cell at the increased background, the count rate was measured of an old Lucas cell (KS-71/85) exhibiting a very high background corresponding to 740 Bq/m^3 of radon concentration. The equivalent background radon concentration was computed from Eq. (10), where the mean background count rate is n=15.1 cpm, and the coefficient k=0.854 for an average count rate in the period

1-180 min. The count rate of the measured background was then added to the raw spectra described in the previous section and such spectra were PCR processed with one principal component. The results of computations are shown in Fig. 16 and are given in Table 7.

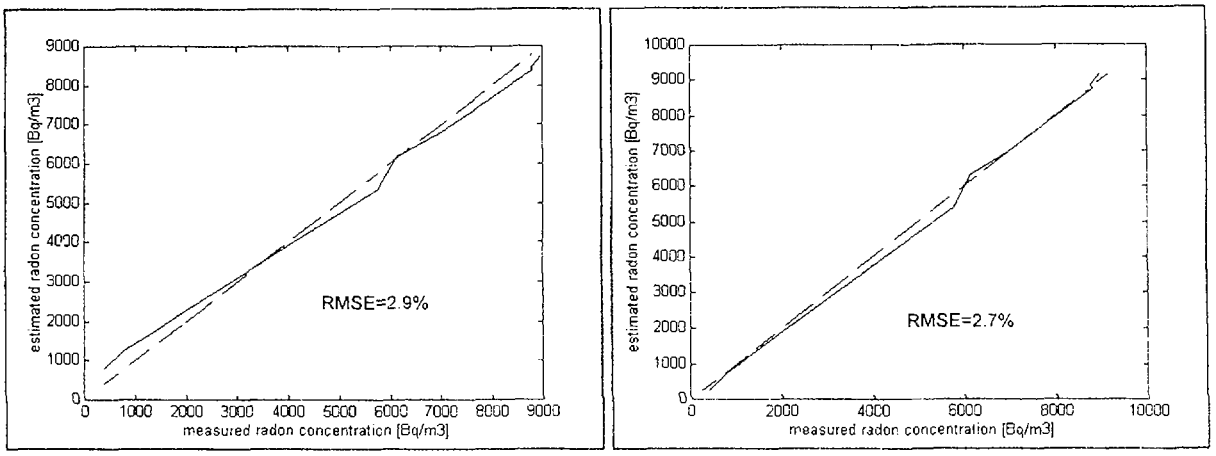

Fig. 16. PCR processed (raw) count rate with zero background (left) and 740 Bq/m^3 background (right).

To investigate the random error caused by the background count rate, the spectra x_0 (without background) were summed with the background spectrum with a random time shift with respect to the x_0 spectra (Appendix 8). The results of 10 computations are shown in Table 8 and in column 4 of Table 7.

Table 8. Estimated (computed) radon concentration in Bq/m^3 for background signal delayed by different time with respect to x_0 spectra. Last row gives an average value and standard deviation of radon concentration.

y1	y2	y3	y4	y5	y6	y7	y8	y9	y10
255	741	1153	1834	5373	6294	6960	8750	8850	9190
253	740	1152	1837	5372	6296	6961	8751	8848	9190
254	740	1153	1834	5371	6295	6961	8753	8848	9192
251	739	1156	1834	5371	6295	6962	8749	8852	9196
251	741	1154	1832	5369	6294	6961	8753	8856	9197
252	741	1152	1832	5370	6297	6960	8755	8859	9196
252	739	1151	1832	5372	6294	6965	8760	8858	9199
250	738	1151	1835	5369	6299	6970	8759	8861	9199
249	738	1153	1831	5374	6304	6970	8762	8861	9198
249	739	1150	1835	5378	6305	6973	8762	8860	9199
251 ±2.0	739 ±1.2	1152 ±1.7	1833 ±1.8	5371 ±2.7	6297 ±3.9	6964 ±4.9	8755 ±5.0	8855 ±5.3	9195 ±3.6

Conclusions that can be drawn from the above computation are the following:

- For once calibrated gauge on the basis of count rate spectra x_0 at no background (count rate =0), the regression coefficients b are achieved and the radon concentration is computed from the relation: $y = b_0 + x_0 * b'$.
- With the background equivalent to 740 Bq/m^3, the radon concentration is determined employing the same regression coefficients b, only b_0 is corrected by the mean background (740 Bq/m^3), with standard deviation ≤2 Bq/m^3 at a low (≤1833 Bq/m^3) radon concentration. The standard deviation of the background count rate only, without PCR processing, is equal to $\sqrt{15.1/180} = 0.29$ cpm, which corresponds to the standard deviation of the radon concentration 14 Bq/m^3. PCR processing ensures thus a considerable (≥7 times) reduction of random error due to the background of the Lucas cell.

4.3. Processing of count rate spectra in the range 161-180 minutes

Results of PCR processing of the Lucas cell count rate spectra measured at an interval of 161 to 180 min after the radon had been introduced into the cell are shown in Table 9. Processing of 21x10 spectra (Appendices 9 and 10) for one principal component were carried out, but only 10 results of the estimated radon concentration y_{est} for low radon concentration are presented in the tables. The coefficient b_0 was corrected by the value -660 Bq/m^3 resulting from Eq. (10) and corresponding to the background count rate. The standard deviation shown in the last column of Table 9 was computed in the same way as in the previous case. The background count rate was added to the measured (raw) count rate spectra with a random time shift and such spectra were PCR processed. The procedure was repeated and the standard deviation was computed as shown in Table 10.

Table 9. Estimated radon concentration at zero background and at 660 Bq/m^3 background.

Item	y_0 Bq/m^3	y_{est} from x_0 Bq/m^3	$y_{est} \pm std(y_{est})$ from (x_0+bknd)+corrected b_0 Bq/m^3
1	405	417	436 ± 26.6
2	783	798	800 ± 25.3
3	1224	1242	1239 ± 27.6
4	1937	1960	1944 ± 22.3
5	5757	5497	5473 ± 21.1
6	6134	6143	6117 ± 9.9
7	6962	6977	6947 ± 13,3
8	8798	8807	8789 ± 21.9
9	8792	8814	8803 ± 29,9
10	8979	8984	8986 ± 27.7
b_0	-	10.6	-649.4

Conclusions that can be drawn from the above computation are the following. At the Lucas cell background equivalent to 660 Bq/m^3 the radon concentration is determined employing

Table 10. Readings of radon concentration estimation at 660 Bq/m^3 background, and estimated average concentration and std deviation (last row).

y1 Bq/m^3	y2 Bq/m^3	y3 Bq/m^3	y4 Bq/m^3	y5 Bq/m^3	y6 Bq/m^3	y7 Bq/m^3	y8 Bq/m^3	y9 Bq/m^3	y10 Bq/m^3
471	842	1264	1990	5516	6127	6948	8772	8782	8959
472	809	1266	1965	5497	6122	6947	8783	8763	8949
429	817	1283	1963	5489	6125	6943	8761	8780	8963
439	829	1261	1944	5468	6108	6944	8783	8773	8967
441	803	1242	1938	5468	6119	6925	8772	8797	8973
458	801	1235	1941	5463	6097	6943	8786	8807	9003
436	782	1214	1924	5464	6118	6935	8791	8802	9003
417	776	1213	1935	5446	6108	6959	8797	8839	9023
410	779	1209	1913	5463	6122	6970	8827	8845	9000
389	762	1210	1935	5456	6127	6964	8827	8842	9026
436,2 ±26.6	800 ±25.3	1239 ±27.6	1944 ±22.3	5473 ±21.1	6117 ±9.9	6947 ±13.3	8789 ±21.9	8803 ±29.9	8986 ±27.7

the same regression coefficients b, only b_0 is corrected by the mean background (660 Bq/m^3), with standard deviation ≤30 Bq/m^3. The standard deviation of background count rate only, without PCR processing, is equal to $\sqrt{15.1/20} = 0.87$ cpm which corresponds to the standard deviation of the radon concentration 38 Bq/m^3. The improvement is not so good when the count rate spectra measured at the time interval 1-180 min was PRC processed. Taking into account the standard deviation of the count rate originating from the radon and from the background equal to $\sqrt{24.4/20} = 1.1$, the standard deviation of the corresponding radon concentration is equal to 48 Bq/m^3 which is 1.6 times lower than with PCR processing.

5. CONCLUSIONS

PCR processing of the measured (raw) signal from the radiation detector of the radon decay products concentration improves the lower detection level of the gauge. PCR processing removes a great part of the count rate random fluctuations originating from the radiation statistics. At a low radon daughters concentration the decrease of root mean square error of the count rate measurement is about 3 times, which is equivalent to the lower detection level of the gauge by a factor of 3. Such an increase of the sensitivity without PCR processing would require a 3^2=9 increase of the air flow rate through the air filter.

Similar investigations concerning the use of Lucas cell for the measurement of radon concentration in air showed that PCR processing of raw data decreases approximately 7 times RMSE when the count rate registered in the period 1 to 180 min is PCR processed. In case when the count rate spectra was measured at the time interval 161-180 min, after the air sample had been introduced into the cell, was PCR processed, the improvement was only 1.6 times.

6. REFERENCES

[1]. Gelardi P., Kowalski B.R.: Partial Least Squares regression: a Tutorial. Analytica Chimica Acta, 185, 1-17 (1986).

[2]. Martens H., Naes T.: Multivariate Calibration. Wiley & Sons, Chichester 1991.

[3]. Rencher A.C.: Multivariate statistical inference and application. John Wiley & Sons, New York 1998.

[4]. Gierdalski J., Bartak J., Urbański P.: Nukleonika, 38, 27 (1993).

[5]. Machaj B.: Modification of the RGR monitor of radon daughters concentration in air. Nukleonika, 44, 479-490 (1999).

[6]. Ewans R.D.: The Atomic Nucleous. McGraw-Hill Book Company, 1970, p. 972.

[7]. Wise B.M., Gallager N.B.: PLS_Toolbox version 1.5 for use with MATLAB. 1997.

[8]. Machaj B.: Pomiar koncentracji radonu za pomocą komory Lucasa. Raporty IChTJ. Seria B nr 12/97.

[9]. Machaj B., Urbański P.: Continuous measurement of radon concentration in the air with Lucas cell by periodic sampling. Nukleonika, 44, 579-594 (1999).

APPENDICES

Appendix 1. (program p4.m)

```
% mean count rates and RMSE for RGR radon daughters monitor
% t1=17 min., t2=8-20 min., t3=21-30 min. counting intervals
% x0 contains 49 measured (raw) count rate spectra in 30 channels (minutes)
% xm contains 49 simulated count rate spectra in 30 channels (minutes)
% results of computations is in matrix k
for i=1:49,
  z=x0(i,:)-xm(i,:);
  s1=sum(x0(i,1:7))/7;
  s2=sum(x0(i,8:20))/13;
  s3=sum(x0(i,21:30))/10;
  z1=z.*z;
  ss1=sqrt(sum(z1(1:7))/7);
  ss2=sqrt(sum(z1(8:20))/13);
  ss3=sqrt(sum(z1(21:30))/10);
  k1(i)=s1;k2(i)=s2;k3(i)=s3;kk1(i)=ss1;kk2(i)=ss2;kk3(i)=ss3;
  k0(i)=i;
end
k=[k0' k1' k2' k3' kk1' kk2' kk3'];
clear z1;clear z2;clear s1;clear s2;clear s3;clear ss1;clear ss2;clear ss3;
```

Appendix 2. (program p5.m)

```
% sum of squares of PCR spectrum processed for rgr
% t1=17 min., t2=8-20 min., t3=21-30 min. counting intervals
% xm contains 49 simulated count rate spectra in 30 channels (minutes)
% tp2 contains 49 PCR processed  count rate spectra in 30 channels (minutes)
% results of computation is given in matrix k
for i=1:49,
  z=tp2(i,:)-xm(i,:);
  s1=sum(tp2(i,1:7))/7;
  s2=sum(tp2(i,8:20))/13;
  s3=sum(tp2(i,21:30))/10;
  z1=z.*z;
  ss1=sqrt(sum(z1(1:7))/7);
  ss2=sqrt(sum(z1(8:20))/13);
  ss3=sqrt(sum(z1(21:30))/10);
  k1(i)=s1;k2(i)=s2;k3(i)=s3;kk1(i)=ss1;kk2(i)=ss2;kk3(i)=ss3;
  k0(i)=i;
end
k=[k0' k1' k2' k3' kk1' kk2' kk3'];
clear z1;clear z2;clear s1;clear s2;clear s3;clear ss1;clear ss2;clear ss3;
```

Appendix 3. (program p6.m)

```
% simulated fluctuations of rgr monitor
%  xm - simulated 49 count rate spectra with radon1.pas program
% xr - simulated  49 count rate spectra with random fluctuations added
x=1:30;
for i=1:49,
  z=xm(i,:);
  r=randn(1,30);
  z1=sqrt(z).*r+z;
  z1=round(z1);
  xr(i,:)=z1;
end
```

Appendix 4. (program p7.m)

```
% Root mean square error for spetra with simulated fluctuations for RGR
% monitor and PCR processed
% t1=17 min., t2=8-20 min., t3=21-30 min. counting intervals
% xr contains 49 simulated count rate spectra with random fluctuations
% added in 30 channels (minutes)
% xm contains 49 simulated count rate spectra with radon1.pas program
% tpr2 contains 49 PCR processed count rate spectra in 30 channels (minutes)
% with 2 principal components
% result of computations are given in matrix k
for i=1:49,
  z=tpr2(i,:)-xm(i,:);
  s1=sum(tpr2(i,1:7))/7;
  s2=sum(tpr2(i,8:20))/13;
  s3=sum(tpr2(i,21:30))/10;
  z1=z.*z;
  ss1=sqrt(sum(z1(1:7))/7);
  ss2=sqrt(sum(z1(8:20))/13);
  ss3=sqrt(sum(z1(21:30))/10);
  k1(i)=s1;k2(i)=s2;k3(i)=s3;kk1(i)=ss1;kk2(i)=ss2;kk3(i)=ss3;
  k0(i)=i;
end
k=[k0' k1' k2' k3' kk1' kk2' kk3'];
clear z1;clear z2;clear s1;clear s2;clear s3;clear ss1;clear ss2;clear ss3;
```

Appendix 5. (program p8.m)

```
% RMSE of raw count rate of Lucas cell
% x0 - measured (raw) count rate spectra
% xs - simulated count rate spectra
% k matrix contains results of computations
for i=1:21,
 z=x0(i,:)-xs(i,:);
 s1=sum(x0(i,1:10))/10;
 s2=sum(x0(i,161:180))/20;
 s3=sum(x0(i,1:180))/180;
 z1=z.*z;
 ss1=sqrt(sum(z1(1:10))/10);
 ss2=sqrt(sum(z1(161:180))/20);
 ss3=sqrt(sum(z1(1:180))/180);
 k1(i)=s1;k2(i)=s2;k3(i)=s3;kk1(i)=ss1;kk2(i)=ss2;kk3(i)=ss3;
 k0(i)=i;
end
k=[k0' k1' k2' k3' kk1' kk2' kk3'];
clear z1;clear z2;clear s1;clear s2;clear s3;clear ss1;clear ss2;clear ss3;
```

Appendix 6. (program p9.m)

```
% RMSE of PCR processed raw cout rate spectra of Lucas cell
% x0 measured (raw) count rate spectra
% tp1 PCR processed count rate spectra with 1 principal component
% xs simulated cout rate spectra
% k matrix contains results of comoutations.
for i=1:21,
 z=tp1(i,:)-xs(i,:);
 s1=sum(tp1(i,1:10))/10;
 s2=sum(tp1(i,161:180))/20;
 s3=sum(tp1(i,1:180))/180;
 z1=z.*z;
 ss1=sqrt(sum(z1(1:10))/10);
 ss2=sqrt(sum(z1(161:180))/20);
 ss3=sqrt(sum(z1(1:180))/180);
 k1(i)=s1;k2(i)=s2;k3(i)=s3;kk1(i)=ss1;kk2(i)=ss2;kk3(i)=ss3;
 k0(i)=i;
end
k=[k0' k1' k2' k3' kk1' kk2' kk3'];
clear z1;clear z2;clear s1;clear s2;clear s3;clear ss1;clear ss2;clear ss3;
```

Appendix 7. (program p10.m)

```
% computation of root mean square error of calibration
% x - matrix of independent variables
% y - matrix of dependent variables
% pc -  number of principal components
% bb - matrix of regression coefficients
% rmsec - root mean square error of calibration
% rmsecr - relative root mean square error of calibration
pc=input('pc = ');
[mx,nx]=size(x0);
[my,ny]=size(y0);
if mx~=my
  error('liczba wierszy w macierzy x i y jest rozna')
end
[t,p,b]=pcr(x0,y0,pc);
r=(pc-1)*ny;
bb=b(r+1:r+ny,:);
plot(bb');                    % diagram of regression coefficients
b0=(ones(mx,1)*(mean(y0)-mean(x0)*bb'))
est=b0+x0*bb';
r=(est-y0).*(est-y0);
rmsec=sqrt(sum(r(:,1:ny))./my)
rmsecr=rmsec/mean(est)
```

Appendix 8. (program p11.m)

```
% computation of  RMSEC
% x0 measured spectra
% y0 calibration data
% z0 measured spectra + background (rk42)
x=z0;
y=y0;
[mx,nx]=size(z0)
[my,ny]=size(y0)
[t,p,b]=pcr(x,y,1);
plot(b');
b0=-118.7-740
est=b0+x*b';
r=(est-y).*(est-y);
rmsec=sqrt(sum(r(:,1:ny))./my)
rmsecr=rmsec/mean(y)
```

Appendix 9. (program p11a.m)

```
% RMSEC  computations
% x0 measured spectra
% y0 calibration data
% z0 measured spectra + background (rk42) computed acc to p12.m
x=x0(:,161:180);
y=y0;
[mx,nx]=size(x0(:,161:180));
[my,ny]=size(y0);

[t,p,b]=pcr(x,y,1);
plot(b');
%b0=(ones(mx,1)*(mean(y)-mean(x)*b'))
b0=10.6-660
x=z0(:,161:180);
est=b0+x*b';
r=(est-y).*(est-y);
rmsec=sqrt(sum(r(:,1:ny))./my)
rmsecr=rmsec/mean(y)
```

Appendix 10. (program p12.m)

```
% background count rate summed with the spectra x0 with time shift
% m - time shift
 m=input('m = ');
for i=1:21,
  k=3*i+m;
  z0(i,:)=x0(i,:)+rk42(k:179+k);
end
```